

12



AD-A141 725

A MODEL OF ROTOR BLADE FIRST NATURAL FLAPPING
RESPONSE FOR UP TO THREE/REV EXCITATIONS

by

Joseph B. Wilkerson

APPROVED FOR PUBLIC RELEASE:
DISTRIBUTION UNLIMITED

AVIATION AND SURFACE EFFECTS DEPARTMENT

DTNSRDC/ASED-83/09

December 1983

DAVID
W.
TAYLOR
NAVAL
SHIP
RESEARCH
AND
DEVELOPMENT
CENTER

BETHESDA
MARYLAND
20884

DTIC FILE COPY

DTIC
ELECTE
S JUN 1 1984 D
A [Signature]

This document has been approved
for public release and sale; its
distribution is unlimited.

B4 05 29 014

UNCLASSIFIED

SECURITY CLASSIFICATION OF THIS PAGE (When Data Entered)

REPORT DOCUMENTATION PAGE		READ INSTRUCTIONS BEFORE COMPLETING FORM
1. REPORT NUMBER DTNSRDC/ASED-83/09	2. GOVT ACCESSION NO. A141725	3. RECIPIENT'S CATALOG NUMBER
4. TITLE (and Subtitle) A MODEL OF ROTOR BLADE FIRST NATURAL FLAPPING RESPONSE FOR UP TO THREE/REV EXCITATIONS	5. TYPE OF REPORT & PERIOD COVERED Final Report	
	6. PERFORMING ORG. REPORT NUMBER	
7. AUTHOR(s) Joseph B. Wilkerson	8. CONTRACT OR GRANT NUMBER(s)	
9. PERFORMING ORGANIZATION NAME AND ADDRESS David Taylor Naval Ship R&D Center Aviation and Surface Effects Department Bethesda, Maryland 20084	10. PROGRAM ELEMENT, PROJECT, TASK AREA & WORK UNIT NUMBERS ARPA Order 4238 Program Element 62711E Work Unit 1-1690-102	
11. CONTROLLING OFFICE NAME AND ADDRESS Defense Advanced Research Projects Agency 1400 Wilson Boulevard Arlington, Virginia 22209	12. REPORT DATE December 1983	
	13. NUMBER OF PAGES 24	
14. MONITORING AGENCY NAME & ADDRESS (if different from Controlling Office)	15. SECURITY CLASS. (of this report) UNCLASSIFIED	
	15a. DECLASSIFICATION/DOWNGRADING SCHEDULE	
16. DISTRIBUTION STATEMENT (of this Report) APPROVED FOR PUBLIC RELEASE: DISTRIBUTION UNLIMITED		
17. DISTRIBUTION STATEMENT (of the abstract entered in Block 20, if different from Report)		
18. SUPPLEMENTARY NOTES		
19. KEY WORDS (Continue on reverse side if necessary and identify by block number) Helicopters Circulation Control X-Wing Rotor Dynamics		
20. ABSTRACT (Continue on reverse side if necessary and identify by block number) Thus far, all performance calculations for the X-Wing vertical takeoff concept have used a rigid, nonflapping blade analysis. At this stage in the concept development, the flapping degree of freedom should be included for increased accuracy. Thus, a relatively simple set of equations is developed to relate rotor blade aerodynamic moments and blade flapping response which provides rapid evaluation of the blade dynamics and the resulting changes in (Continued on reverse side)		

SEARCHED
SERIALIZED
JUN 1 1984
A

UNCLASSIFIED

SECURITY CLASSIFICATION OF THIS PAGE (When Data Entered)

Block 20 (Continued)

aerodynamic loading. The relationships between the aerodynamic hinge moments and the blade response are derived for the first three harmonics of flapping. Changes in flap damping due to flapping response are accounted for in the equations, which are solved using standard matrix algebra. The equations are validated by comparison with a more sophisticated analytical technique. A case is examined for the critical conversion advance ratio, and the first-order dynamic response is shown for a range of blade natural frequencies. It is shown that a blade natural frequency higher than 2-per-rev is desired.



Accession For	
NTIS GRA&I	<input checked="" type="checkbox"/>
DTIC TAB	<input type="checkbox"/>
Unannounced	<input type="checkbox"/>
Justification	
Distribution/	
Availability Codes	
Dist	Avail and/or Special
A-1	

UNCLASSIFIED

SECURITY CLASSIFICATION OF THIS PAGE (When Data Entered)

TABLE OF CONTENTS

	Page
LIST OF FIGURES	iii
ABSTRACT	1
ADMINISTRATIVE INFORMATION	1
INTRODUCTION	1
DERIVATION OF EQUATIONS	2
BASIC FLAPPING EQUATION	2
EXTERNAL MOMENTS	3
FLAP DAMPING TERMS	4
HARMONIC SOLUTION	6
XWDYN COMPUTER PROGRAM	8
DESCRIPTION	8
VALIDATION	9
DYNAMIC RESPONSE STUDY	10
PHYSICAL CHARACTERISTICS	10
FLAP FREQUENCY SENSITIVITY	13
NET HINGE MOMENTS	15
APPLICATION TO ROTOR PERFORMANCE ANALYSIS	18
HUB MOMENTS	18
SOLUTION	19
SUMMARY	21

LIST OF FIGURES

1 - Offset Hinge Dynamics Model	1
2 - Change in Angle of Attack Due to Flapping Velocity	5
3 - Inputs and Results for Validation Case	10
4 - Flapping Response for X-Wing Case	12
5 - Approximate Change in Blade Tip Angle of Attack	13
6 - Comparison of Flapping Response for P=1.8 and P=2.2	14
7 - Variation in Flapping Magnitude and Phase Angle with Flap Frequency	16
8 - Variation of One/Rev Net Hinge Moments with Flap Frequency	17
9 - Cross Plot of Net Hinge Moment Components	18
10 - Modular Inclusion of Rotor Blade Dynamics	20

ABSTRACT

Thus far, all performance calculations for the X-Wing vertical takeoff concept have used a rigid, nonflapping blade analysis. At this stage in the concept development, the flapping degree of freedom should be included for increased accuracy. Thus, a relatively simple set of equations is developed to relate rotor blade aerodynamic moments and blade flapping response which provides rapid evaluation of the blade dynamics and the resulting changes in aerodynamic loading. The relationships between the aerodynamic hinge moments and the blade response are derived for the first three harmonics of flapping. Changes in flap damping due to flapping response are accounted for in the equations, which are solved using standard matrix algebra. The equations are validated by comparison with a more sophisticated analytical technique. A case is examined for the critical conversion advance ratio, and the first-order dynamic response is shown for a range of blade natural frequencies. It is shown that a blade natural frequency higher than 2-per-rev is desired.

ADMINISTRATIVE INFORMATION

The work presented herein was conducted at the David W. Taylor Naval Ship Research and Development Center (DTNSRDC) for the Defense Advanced Research Projects Agency under ARPA order 4238, DTNSRDC Work Unit 1-1690-102.

For this evaluation all dimensions were either measured in or converted directly to U.S. customary units. Hence, U.S. customary units are the primary units in this report. Angular measurement is in radians except where degrees are specified.

INTRODUCTION

The importance of blade dynamics to the analysis of helicopter performance and control has long been recognized. Ongoing development of the circulation control rotor technology and application to the high-speed X-Wing aircraft have concentrated on the unique aerodynamic characteristics of these rotor systems. Early X-Wing designs had very stiff blades, and an assumption of perfectly rigid blades was made to simplify analysis. However, interaction between the rotor aerodynamics and blade dynamics does modify the control phase angles for trim and

the resultant hub moment responses to control inputs, especially on designs having lower flapping stiffness. Both items, therefore, are highly important to the overall rotor and control system design and to the subsequent analysis of performance and control sensitivity.

The blade dynamics model must be easily incorporated into the existing rigid-blade aerodynamic analysis. An approach, therefore, was taken to develop a separate blade dynamics module. This module uses aerodynamic hinge moments from the main analysis, in the form of Fourier series coefficients, to calculate the first three harmonics of blade flapping response. The blade dynamics model is that of a rigid blade with offset hinge and spring restraint, thus modeling only the first natural flapping mode of the blade. Since the module includes the first-order dynamic terms of mass, inertia, and centrifugal force effects, these terms are not required in the main program. The module also includes aerodynamic flap damping terms to reflect changes (up to three harmonics) that arise from the difference between the reference flapping and the calculated resultant flapping response. Aerodynamic damping due to the reference flapping is assumed to be included in the aerodynamic hinge moments provided. Output from the module is simply the Fourier series coefficients of the resultant blade dynamic flapping response. These coefficients are then used in the existing aerodynamic analysis to account for the influence of blade flapping position and velocity on the local angle of attack and to properly resolve hub moments back through the flapping hinge.

As a part of this program development effort, the dynamics module was used in a preliminary study of the potential influence of blade dynamics on the X-Wing rotor. The results of this study are presented in this report.

DERIVATION OF EQUATIONS

A simple relationship is developed between blade hinge moments and blade flapping response, based on the first three harmonics of airload versus azimuth. The relationship is intended for use in conjunction with a rotor aerodynamic analysis to account for the influence of blade dynamics on the rotor control requirements and the proper control phase angles for trim and maneuver.

BASIC FLAPPING EQUATION

The fundamental blade dynamic relationship is given by:

$$I\ddot{\beta} + c\dot{\beta} + k\beta = M_e \quad (1)$$

where β = flap angle, radians
 $\ddot{\beta}, \dot{\beta}$ = time derivatives of β
 I = mass moment of inertia of blade about hinge
 c = damping constant
 k = hinge spring constant
 M_e = all external moments

Equation (1) describes the system shown in Figure 1. The three sources of external moments are: (1) distributed lift forces, (2) distributed centrifugal forces, and (3) distributed blade weight.

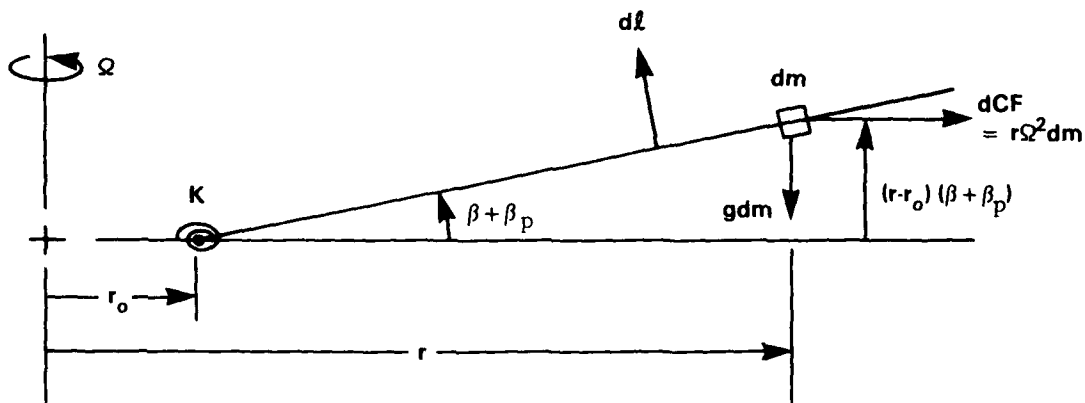


Figure 1 - Offset Hinge Dynamics Model

EXTERNAL MOMENTS

The external moments about the hinge are expressed in integral form as:

$$M_e = \int_{r_o}^R (r-r_o)(dl/dr)dr - \int_{r_o}^R (r-r_o)(\beta+\beta_p) r\Omega^2 (dm/dr)dr - g \int_{r_o}^R (r-r_o)(dm/dr)dr$$

where r_o = hinge offset from centerline of rotation, ft
 Ω = rotational speed, rad/sec
 β_p = precone angle, radians
 β = flapping degree of freedom, radians

Because $d\ell$ and β are both azimuth dependent, the value of M_e is also azimuth dependent. The first integral (lift) is assumed to be available from an aerodynamic analysis as a function of azimuth, $M_h(\psi)$. The second integral (β dependent) and third integral may be expressed in more convenient terms as:

$$M_e = M_h(\psi) - \Omega^2(\beta + \beta_p)(I + r_o \sigma m) - mg\sigma \quad (2)$$

where $M_h(\psi)$ = aerodynamic hinge moment from distributed lift forces
 σ = center-of-gravity location of hinged blade measured from hinge, ft
 m = mass of hinged blade, slugs

Combining Equations (1) and (2) and dividing through by the term $I\Omega^2$ yields the following equation to be solved:

$$\frac{\ddot{\beta}}{\Omega^2} + \gamma \frac{P\dot{\beta}}{\Omega} + P^2\beta = \frac{M_h(\psi)}{I\Omega^2} - \beta_p \left(1 + \frac{r_o \sigma m}{I}\right) - \frac{mg\sigma}{I\Omega^2} \quad (3)$$

where $P = \omega_n / \Omega$, first flap frequency ratio

$$(\omega_n / \Omega)^2 = 1 + \frac{r_o \sigma m}{I} + \frac{k}{I\Omega^2}$$

γ = structural damping factor
 (= 2ζ , two times viscous damping coefficient)

FLAP DAMPING TERMS

Local blade angle of attack is changed by blade flapping response, as depicted in Figure 2. The amount of flap damping due to the reference flapping condition at the time $M_h(\psi)$ was calculated is included in the $M_h(\psi)$ term of Equation (2). The new flapping solution will have a different amount of flap damping, and the difference may be calculated from:

$$\Delta\alpha = \tan^{-1} (w/u) \quad (4)$$

$$\approx -(r - r_o) \Delta\dot{\beta} / u$$

where $\Delta\dot{\beta}$ is the difference between the new solution flap rate and the reference flapping condition, and u is the local velocity vector. The aerodynamic angle of attack (hence, load) and blade flapping are interdependent.

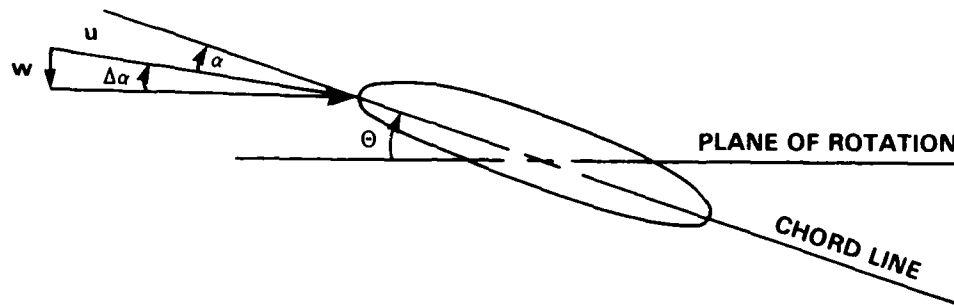


Figure 2 - Change in Angle-of-Attack Due to Flapping Velocity

This projected change in flap damping hinge moment due to the change in angle of attack is represented by:

$$\Delta M_h = \int_{r_0}^R (r-r_0) a \Delta\alpha q c dr \quad (5)$$

Equation (5) can be evaluated by substituting Equation (4) for $\Delta\alpha$. The u term in the denominator of Equation (4) partially cancels the dynamic pressure q of Equation (5). The c term in Equation (5) can be approximated by the mean aerodynamic chord, and the remaining u term can be approximated by the local in-plane velocity. To properly reflect damping in the reverse flow region, u should be taken as an absolute value. But to keep the algebra solvable, the absolute value has been dropped, yielding an inaccurate estimate of the damping change in the reverse flow region. This approximation does not influence the aerodynamic damping included in the $M_h(\psi)$ term of Equation (3), which correctly reflects all aerodynamic terms from a separate analysis; therefore, the approximation does not affect the converged flapping solution. However, the rate of flapping convergence for very high advance ratios may be influenced. Even at an advance ratio of one, the advancing blade damping is still an order of magnitude

greater than the retreating blade damping. Thus the harmonic content of the damping term is only weakly influenced by the reverse flow region. Performing the radial integration then gives a relationship between ΔM_h and the flapping solution.

$$\Delta M_h = - (1/2) \gamma_L I \Omega (F_1 + \mu F_2 \sin \psi) (\dot{\beta} - \dot{\beta}_{ref}) \quad (6)$$

where $\gamma_L = \text{Lock number } (\rho a c R^4 / I)$

$a = \text{lift curve slope}$

$$F_1 = 1/4 - 2x_o/3 + x_o^2/2 - x_o^4/12$$

$$F_2 = 1/3 - x_o + x_o^2 - x_o^3/3$$

$$x_o = r_o/R$$

Equation (6) represents a change in the external moment beyond the $M_h(\psi)$ value of Equation (3). The term $\Delta M_h / (I \Omega^2)$, therefore, must be added to the right-hand side of Equation (3) to include the projected flap damping terms.

$$\frac{\ddot{\beta}}{\Omega^2} + \gamma \frac{P \dot{\beta}}{\Omega} + P^2 \beta = \frac{M_h(\psi)}{I \Omega^2} + \frac{\Delta M_h}{I \Omega^2} - \beta_p (1 + r_o \sigma m / I) - \frac{mg \sigma}{I \Omega^2} \quad (7)$$

The change in the external hinge moment is proportional to the difference between the reference flapping and the flapping solution ($\dot{\beta} - \dot{\beta}_{ref}$). As dynamic and aerodynamic solutions converge, the term ($\dot{\beta} - \dot{\beta}_{ref}$) approaches zero, as does the projected flap damping in Equation (6). Thus, the converged solution is unaffected by the previously mentioned approximations used in deriving the equation.

HARMONIC SOLUTION

The simple harmonic solution of Equation (7) is obtained in four steps:

1. The $M_h(\psi)$ term is assumed to be a Fourier Series:

$$\begin{aligned} M_h(\psi) = & M_o + M_{1s} \sin \psi + M_{1c} \cos \psi \\ & + M_{2s} \sin 2\psi + M_{2c} \cos 2\psi \\ & + M_{3s} \sin 3\psi + M_{3c} \cos 3\psi \end{aligned} \quad (8)$$

2. The solution for β also is assumed to be a Fourier series:

$$\begin{aligned}\beta = & \beta_0 + \beta_{1s} \sin \psi + \beta_{1c} \cos \psi \\ & + \beta_{2s} \sin 2\psi + \beta_{2c} \cos 2\psi \\ & + \beta_{3s} \sin 3\psi + \beta_{3c} \cos 3\psi\end{aligned}\tag{9}$$

3. The $\dot{\beta}$ and $\ddot{\beta}$ series are obtained by differentiating the β series.

4. These series are substituted into Equation (7) and coefficients of like terms are equated.

This procedure yields the following matrix formulation for the harmonic solution of the flapping coefficients in Equation (9) in terms of the excitation coefficients from Equation (8):

$$A\{B\} = \{M\}\tag{10}$$

where

$$\{B\} = \begin{Bmatrix} \beta_0 \\ \beta_{1s} \\ \beta_{1c} \\ \beta_{2s} \\ \beta_{2c} \\ \beta_{3s} \\ \beta_{3c} \end{Bmatrix} \quad \text{column array of flapping solution harmonics}$$

and

$$\{M\} = \left\{ \begin{array}{l} M_o^1 - \beta_p \left(1 + \frac{m r_o \sigma}{I}\right) - \frac{mg\sigma}{I\Omega^2} - \frac{1}{4} \gamma_L F_2^\mu \beta_{1c}^* \\ M_{1s}^1 - \frac{1}{2} \gamma_L (F_1 \beta_{1c}^* + F_2^\mu \beta_{2s}^*) \\ M_{1c}^1 - \frac{1}{2} \gamma_L (-F_1 \beta_{1s}^* + F_2^\mu \beta_{2c}^*) \\ M_{2s}^1 - \frac{1}{2} \gamma_L (2F_1 \beta_{2c}^* - \frac{1}{2} F_2^\mu \beta_{1s}^* + \frac{3}{2} F_2^\mu \beta_{3s}^*) \\ M_{2c}^1 - \frac{1}{2} \gamma_L (-2F_1 \beta_{2s}^* - \frac{1}{2} F_2^\mu \beta_{1c}^* + \frac{3}{2} F_2^\mu \beta_{3c}^*) \\ M_{3s}^1 - \frac{1}{2} \gamma_L (3F_1 \beta_{3c}^* - F_2^\mu \beta_{2s}^*) \\ M_{3c}^1 - \frac{1}{2} \gamma_L (-3F_1 \beta_{3s}^* - F_2^\mu \beta_{2c}^*) \end{array} \right\}$$

= column array of external moment harmonics

Here

M_{ns}^1, M_{nc}^1 = coefficients of the $\sin(n\psi)$ and $\cos(n\psi)$ terms, respectively,
from Equation (8) divided by $(I\Omega^2)$

$\beta_{ns}^*, \beta_{nc}^*$ = coefficients of the harmonic terms of the reference flapping
condition

n = harmonic number (1, 2, or 3)

Also,

$$A = \left[\begin{array}{ccccccc} a_{11} & 0 & a_{13} & 0 & 0 & 0 & 0 \\ 0 & a_{22} & a_{23} & a_{24} & 0 & 0 & 0 \\ 0 & a_{32} & a_{33} & 0 & a_{35} & 0 & 0 \\ 0 & a_{42} & 0 & a_{44} & a_{45} & a_{46} & 0 \\ 0 & 0 & a_{53} & a_{54} & a_{55} & 0 & a_{57} \\ 0 & 0 & 0 & a_{64} & 0 & a_{66} & a_{67} \\ 0 & 0 & 0 & 0 & a_{75} & a_{76} & a_{77} \end{array} \right]$$

where

$$\begin{aligned} a_{11} &= P^2, & a_{13} &= -\gamma_L F_2 \mu / 4 \\ a_{22} &= P^2 - 1, & a_{23} &= -(\gamma P + \gamma_L F_1 / 2), & a_{24} &= -\gamma_L F_2 \mu / 2 \\ a_{33} &= P^2 - 1, & a_{32} &= (\gamma P + \gamma_L F_1 / 2), & a_{35} &= -\gamma_L F_2 \mu / 2 \\ a_{44} &= P^2 - 4, & a_{45} &= -2(\gamma P + \gamma_L F_1 / 2), & a_{42} &= \gamma_L F_2 \mu / 4, & a_{46} &= -3\gamma_L F_2 \mu / 4 \\ a_{55} &= P^2 - 4, & a_{54} &= +2(\gamma P + \gamma_L F_1 / 2), & a_{53} &= \gamma_L F_2 \mu / 4, & a_{57} &= -3\gamma_L F_2 \mu / 4 \\ a_{66} &= P^2 - 9, & a_{67} &= -3(\gamma P + \gamma_L F_1 / 2), & a_{64} &= \gamma_L F_2 \mu / 2 \\ a_{77} &= P^2 - 9, & a_{76} &= +3(\gamma P + \gamma_L F_1 / 2), & a_{75} &= \gamma_L F_2 \mu / 2 \end{aligned}$$

Equation (10) is then solved by standard matrix methods to yield the solution vector {B}. Note that the first equation represented in the matrix set is that of the flap coning angle, β_0 . This equation may be decoupled from the rest, leaving only a 6 by 6 matrix, for some savings in computation time. The β_0 term can then be written as a separate algebraic expression in terms of β_{1c} , to which it is coupled.

XWDYN COMPUTER PROGRAM

DESCRIPTION

The harmonic solution is programmed in Basic 2.0 to run on an HP-9836 desktop computer. This program has fixed inputs to represent (1) the blade dynamic characteristics, (2) the aerodynamic hinge moments versus azimuth as a Fourier series, and (3) the initial blade flapping angle versus azimuth as a Fourier series. The solution is a direct application of Equation (10).

VALIDATION

The X-Wing dynamics module XWDYN was validated against a rotor blade dynamics solution from the Circulation Control Rotor Performance Program, CCRPERF. The CCRPERF program solves blade dynamics by azimuthal integration of the coupled flap-lag degrees of freedom until a harmonic solution is obtained, i.e., dynamic

parameters at the end of a revolution are nearly the same as those at the beginning of the revolution.

There are several significant differences between the two dynamics models. First, XWDYN is restricted to only the first three harmonics; whereas, CCRPERF is not restricted. Second, XWDYN is for flapping only; whereas, CCRPERF yields a solution to the coupled two degree-of-freedom flap-lag problem. Third, the CCRPERF integration assumes that aerodynamics are constant over the azimuth interval; whereas, XWDYN takes a continuous Fourier series representation for aerodynamics. Finally, the CCRPERF model accounts for kinematic pitch-flap coupling (δ_3), which introduces changes in the effective stiffness of the blade. As an isolated routine, XWDYN does not account for pitch-flap coupling, but includes that influence as reflected in the input aerodynamic hinge moments.

A validation case was run on the CCRPERF program. The trim condition was chosen to have non-zero hub moments to ensure some blade flapping response. Aerodynamic hinge moments and corresponding blade flapping conditions were taken from the converged CCRPERF solution and used as input to the XWDYN routine. Calculated flapping response from XWDYN must match that from CCRPERF to validate the XWDYN program.

Typical output from the computer runs is shown in Figure 3. The aerodynamic hinge moments and reference flapping condition are specified input parameters. The XWDYN solution results in a 1/rev flapping magnitude within 2.7 percent, and a phase angle within 1.5 deg, of the CCRPERF 1/rev flapping. Considering the above-mentioned differences between the two dynamic analyses, the validation comparison shows good agreement between the CCRPERF reference flapping condition and the XWDYN flapping solution.

DYNAMIC RESPONSE STUDY

The XWDYN module was applied to an X-Wing case to evaluate the module's influence on the "rigid" blade aerodynamics. These results are significant in the relative changes from case to case as well as in the differences from the reference "rigid" case. However, accurate solutions for the amount of flapping require that XWDYN be coupled with a complete aerodynamics model to provide an iterative solution of flapping, aerodynamic loads, and hinge moments.

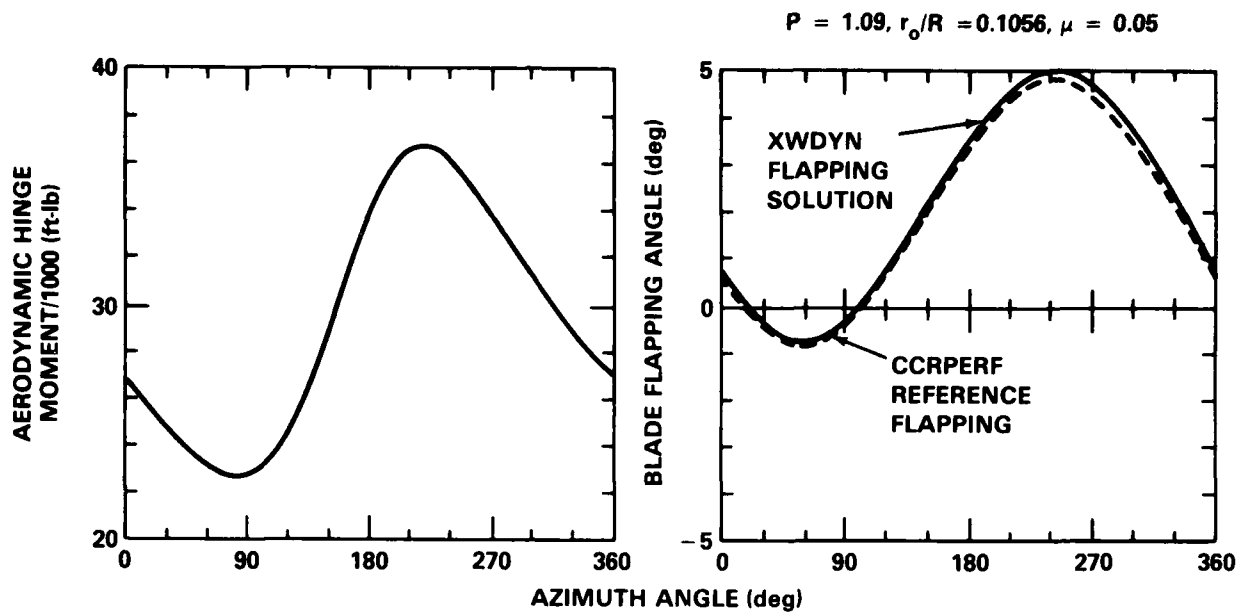


Figure 3 - Inputs and Results for Validation Case

PHYSICAL CHARACTERISTICS

The X-Wing case chosen was that of a full-scale, 50-ft-diameter rotor operating at 0.7 advance ratio. The aerodynamic hinge moments were calculated at DTNSRDC about a 34-percent offset hinge. The rotor was intentionally out-of-trim to provide a non-zero flapping solution. Pertinent parameters for the case are:

Thrust	12,145 lb
Hub Roll	3,666 ft-lb
Hub Pitch	11,253 ft-lb
Shaft Angle	+6 deg
Collective Pitch	-5 deg
Cyclic Pressure	(in terms of pressure ratio)
$\sin(\psi)$	-0.25
$\cos(\psi)$	0.00

From these parameters, it is evident that the positive hub roll is due to the combination of negative $\sin(\psi)$ control input and collective pitch setting; whereas, the positive hub pitch is a result of positive shaft angle and zero $\cos(\psi)$ control input. These observations for the rigid rotor case are important for a later interpretation of the dynamic responses.

Dynamic characteristics are those of a typical, 50 ft-diameter X-Wing design. Mass and inertia terms were estimated from structural requirements based on the 34-percent hinge offset. Typical output for the design flapping frequency case $P = 1.577$ is shown in Figure 4. The most obvious feature of the graph is the dominant 2/rev flapping content. This is consistent with the large 2/rev content from the aerodynamic hinge moment. The curves in Figure 4 illustrate the importance of including the projected aerodynamic flap damping terms in the solution. The curve without projected flap damping shows a much larger 2/rev content than the curve with projected flap damping. The projected flap damping is attributable to the change in flapping from the reference flapping state. In the sample case, these X-Wing aerodynamic loads are from a nondynamic model with zero reference flapping. Thus, all of the aerodynamic flap damping present in the solution shown in Figure 4 was added by the XWDYN program.

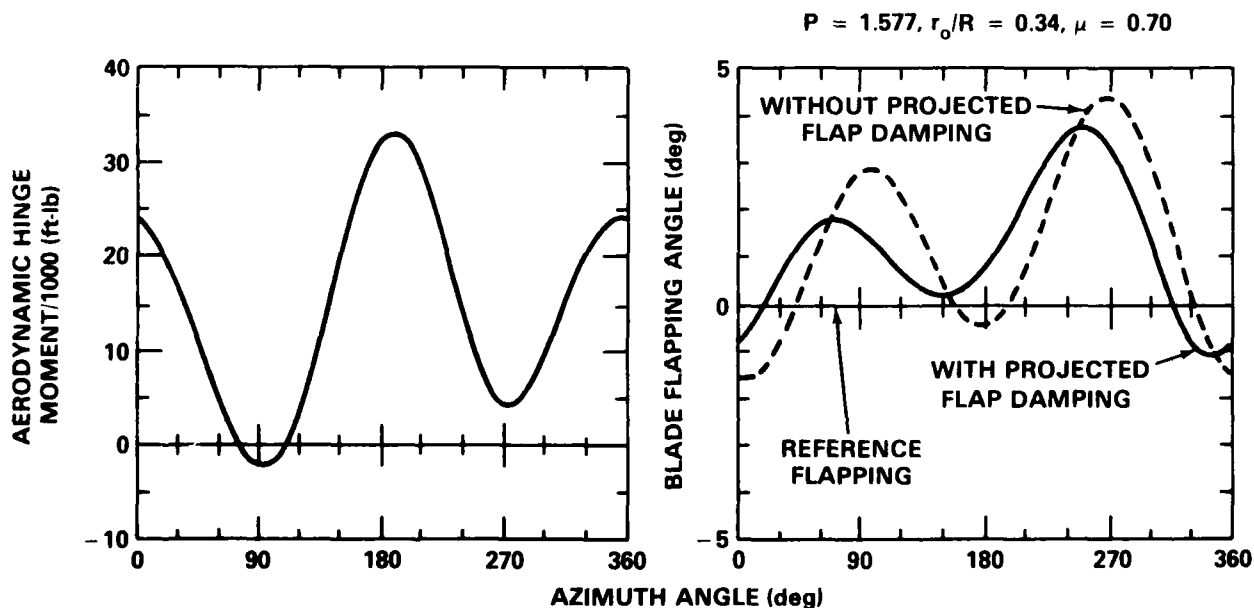


Figure 4 - Flapping Response for X-Wing Case

The potential influence of flapping motion may be estimated from the corresponding change in blade element angle of attack. An approximation of the change in blade tip angle of attack was made using Equation (4) and is shown versus rotor azimuth angle in Figure 5. For $\psi = 0$ to 180 deg, the change is moderate, oscillating about ± 1 deg; however, much larger changes in angle of attack are evident at other azimuth angles. These changes range from -4 deg at $\psi = 220$ to +9 deg at $\psi = 290$ deg, which suggests that flapping motion, even though small, strongly influences aerodynamic loads.

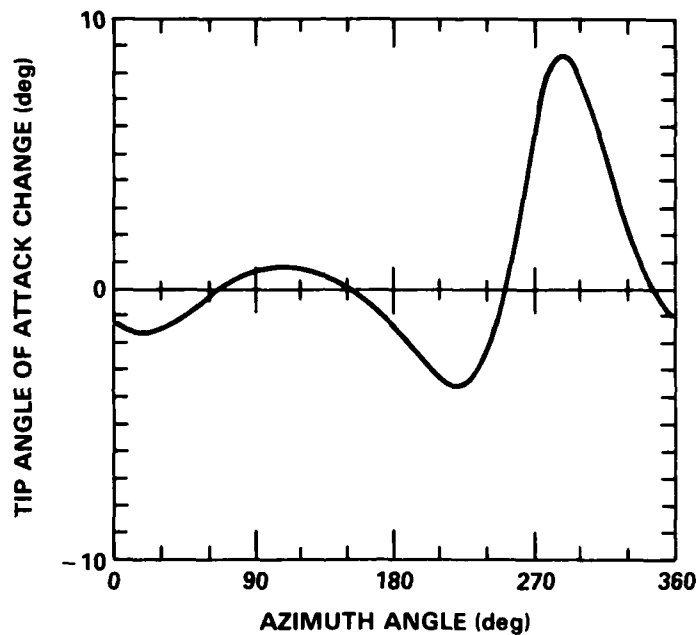


Figure 5 - Approximate Change in Blade Tip Angle of Attack

FLAP FREQUENCY SENSITIVITY

The sample solution described was performed over a range of blade flap frequency ratios to examine the degree of variation in blade response. All other values were held constant during the flap frequency changes. Input aerodynamics were originally from a nondynamic rotor analysis and, therefore, should apply equally well to all cases. The blade hinge offset and the mass and inertia properties were held constant as originally calculated for the flap frequency ratio case; see Figure 4. Thus, the frequency increases must be considered a result of increased hinge spring stiffness.

Results of this study show that flap frequency has a profound influence on the character of flapping response. Flap frequency also can significantly alter the aerodynamic load distributions from those of a "rigid" blade, nondynamic model (at least for the $\mu = 0.7$ case with non-zero hub moments considered here). The 1/rev content of net hinge moment is also modified considerably. However, the net effect of flapping motion on hub trim moments must be determined by the more complete math model.

One example of the flap frequency influence on loads occurs as the blade frequency crosses the 2/rev boundary. A simple, single degree-of-freedom (mass, spring, damper) system will change the phase lag of its response when the excitation frequency goes from below system natural frequency to above system natural frequency. This also holds true for the rotor blade response as its first natural flapping frequency is moved (analytically) about. Figure 6 shows blade flapping response for flapping frequency ratios of 1.8P and 2.2P. The undamped flapping response (dash curves) is dominantly a $\cos(2\psi)$ content, which dramatically changes sign between the 1.8P case and the 2.2P case. The damped response, however, behaves in a much more benign manner, with no change in 2/rev magnitude and only a 25-deg change in 2/rev phase angle. Here again is vivid evidence of the important role damping plays in predicting blade dynamic response during conversion and hence its importance in loads and vibrations. The stiffness increase also yields a substantial (5:1) reduction in the 1/rev flapping magnitude (not readily visible from the figure). These combined influences reduce the 1/rev net hinge moment of the 2.2P case to only 40 percent of that for the 1.8P case.

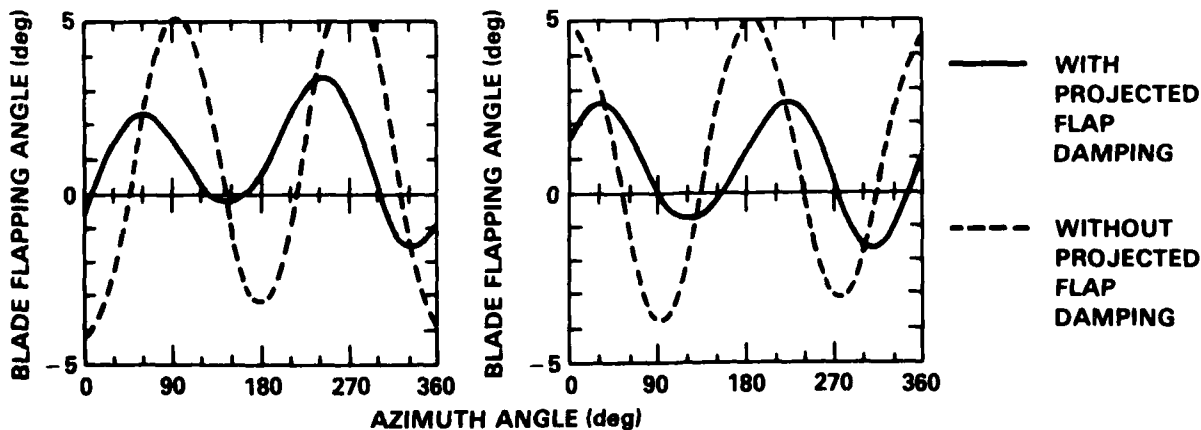


Figure 6a - P = 1.8

Figure 6b - P = 2.2

Figure 6 - Comparison of Flapping Response for P=1.8 and P=2.2

The variation in overall flapping response with changing frequency ratio is summarized in Figure 7. Flap angle magnitude and azimuth angle at maximum flap are shown for each of the first three harmonics over a range of frequency ratios. The curves are extended to a frequency ratio of 10, where the "rigid" blade solution is plotted. The dominate 2/rev response rapidly diminishes as the blade natural frequency ratio extends beyond 2.3/rev. The limited amplitude response at resonance (2-P crossing) reflects a significant (flap) damping content. The phase angle of the 2/rev response shows a gradual shift, leveling out as the blade flap frequency ratio approaches 3/rev. The 3/rev flapping magnitude maintains a moderate level until the blade flap frequency ratio goes beyond 3/rev. This resonant response near 3/rev is somewhat academic because the 3P crossing will only occur at a reduced rotor rpm, and hence at a higher advance ratio than that of these cases. Thus, the aerodynamic loads at $\mu = 0.7$ do not apply. The case is still useful, however, as a check on the validity of the approach.

The 1 P flap response shown in Figure 7 is indicative of control response in that the magnitude of the 1 P net hinge moments passed to the hub are proportional to the 1 P flapping magnitude. This results in a steady moment applied to the airframe. The 1 P flapping content rapidly diminishes as flap frequency ratio increases to a ratio of about 2.2/rev. This is followed by a 90-deg phase shift (at nearly constant amplitude) as the flap frequency ratio increases to about 2.6/rev.

NET HINGE MOMENTS

The net hinge moment at each azimuth is calculated from the product of hinge spring stiffness and flap angle deflection for each azimuth. Thus, the 1/rev content of the net hinge moment is obtained by direct multiplication of the spring stiffness by the 1/rev flapping content. The relation that this net moment has to total hub moment varies with shear load at the hinge and any aerodynamic loads inboard of the hinge. Still, it is of interest to observe the net hinge moment as it varies with flap frequency ratio, because the net hinge moment is a major portion of the total hub moment and vehicle trim moments.

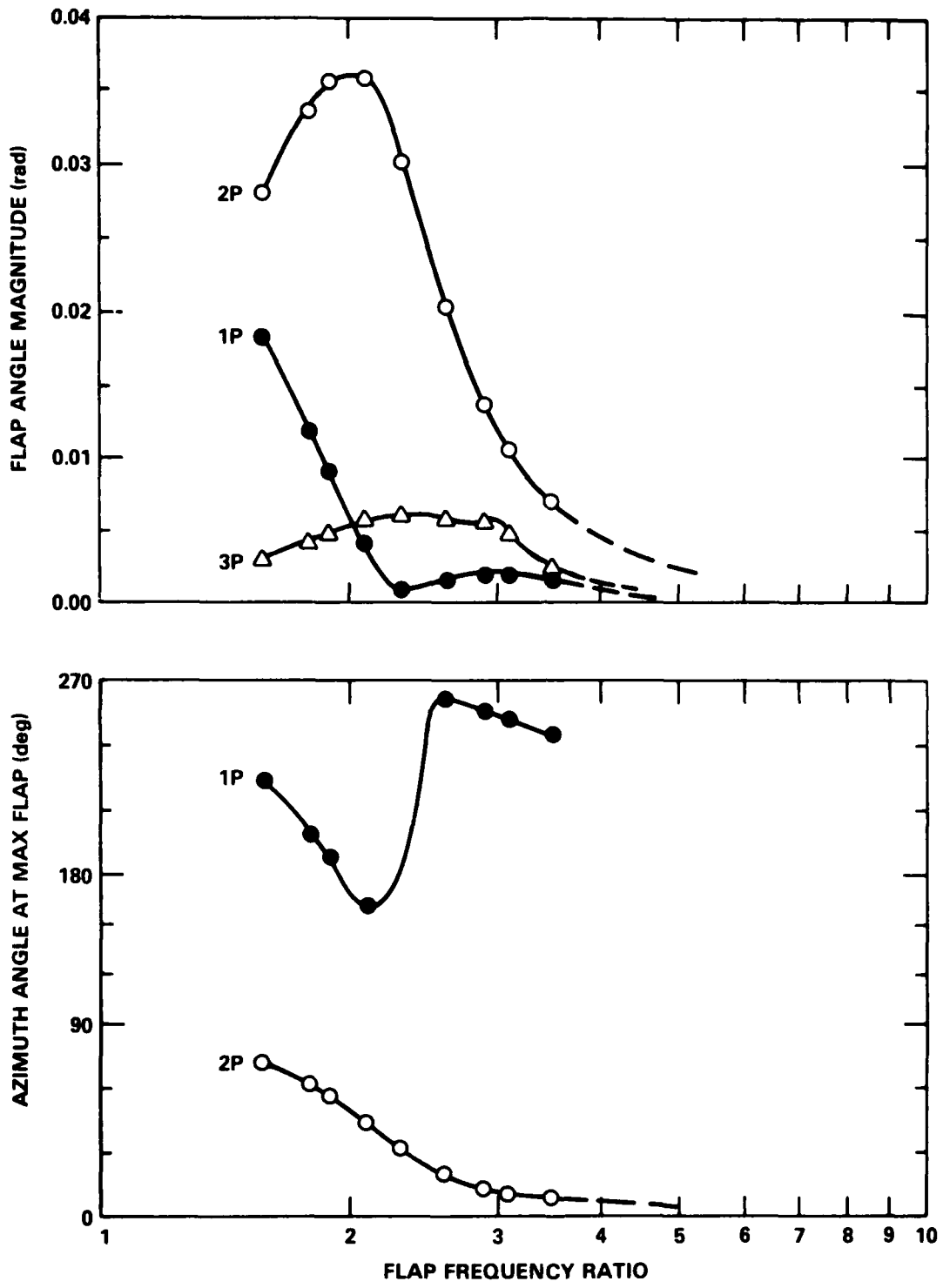


Figure 7 - Variation in Flapping Magnitude and Phase Angle with Flap Frequency

Figure 8 shows the sine and cosine components of 1/rev net hinge moment versus flap frequency ratio. Note that net hinge moment must approach zero as the spring stiffness approaches zero, regardless of the flap angle magnitude. The "rigid" blade values are plotted at a frequency ratio of 10. As stated, the negative $\sin\psi$ pneumatic control input (and collective pitch setting) creates a negative $\sin\psi$ aerodynamic hinge moment. As shown in Figure 8, the $\sin\psi$ component of net hinge moment is always of lower magnitude than that of the rigid blade. The lowest frequency ratio of 1.577 yields about a 2:1 reduction in net hinge moment, suggesting some reduction in roll control effectiveness. For the "rigid" blade case, there is no $\cos\psi$ pneumatic control input, but there is a negative $\cos\psi$ aerodynamic hinge moment arising from the positive shaft angle. This yields a strong pitch-up hub moment. The $\cos\psi$ component of net hinge moment varies considerably with flap frequency ratio.

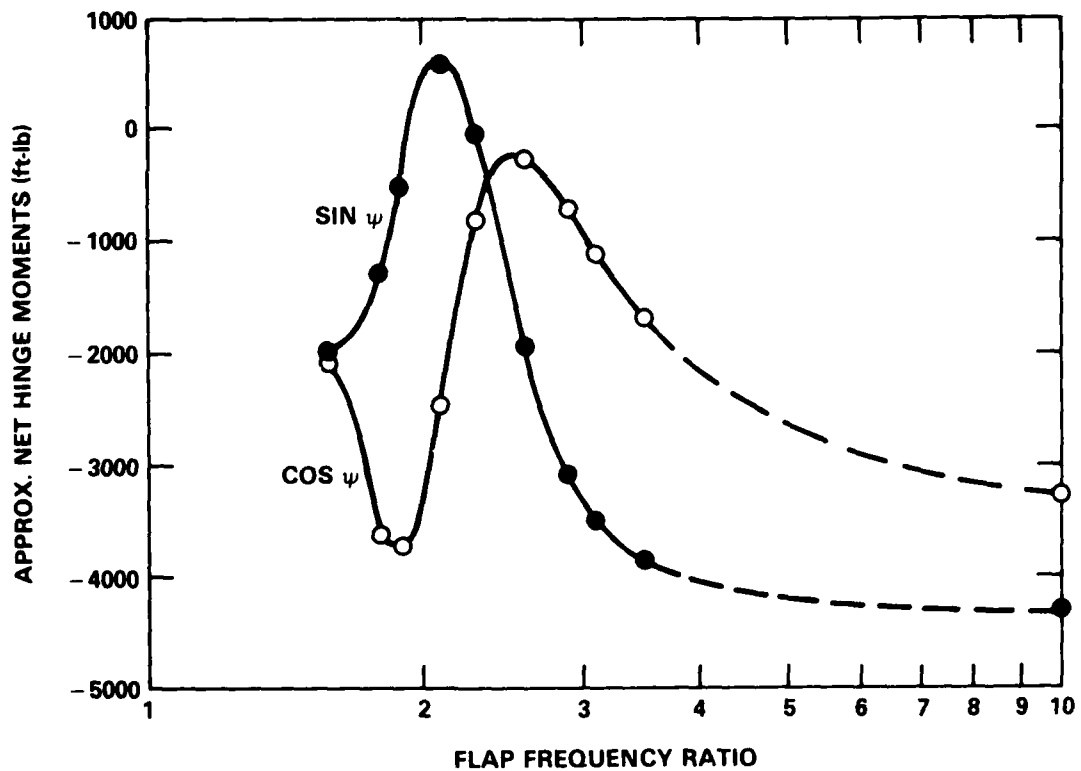


Figure 8 - Variation of One/Rev Net Hinge Moments with Flap Frequency

Net hinge moment is shown in Figure 9 as a cross plot of the $\cos\psi$ versus $\sin\psi$ components with flap frequency as a parameter. The $\sin\psi$ and $\cos\psi$ net hinge moments have a consistent trend toward the "rigid" blade values as frequency is increased. Figure 9 shows that the most $\sin\psi$ response for a $\sin\psi$ control input and the least $\cos\psi$ response for no $\cos\psi$ control input occur in the 2.6/rev to 2.9/rev range of flap frequency ratio. Conversely, the minimum $\sin\psi$ response and the most netative $\cos\psi$ response tend to occur near the 2/rev frequency ratio. These responses are about -90 deg out of phase with the pneumatic control input signal. The best 1/rev control response, therefore, is judged to occur for flap frequency ratios in the 2.6/rev to 2.9/rev range.

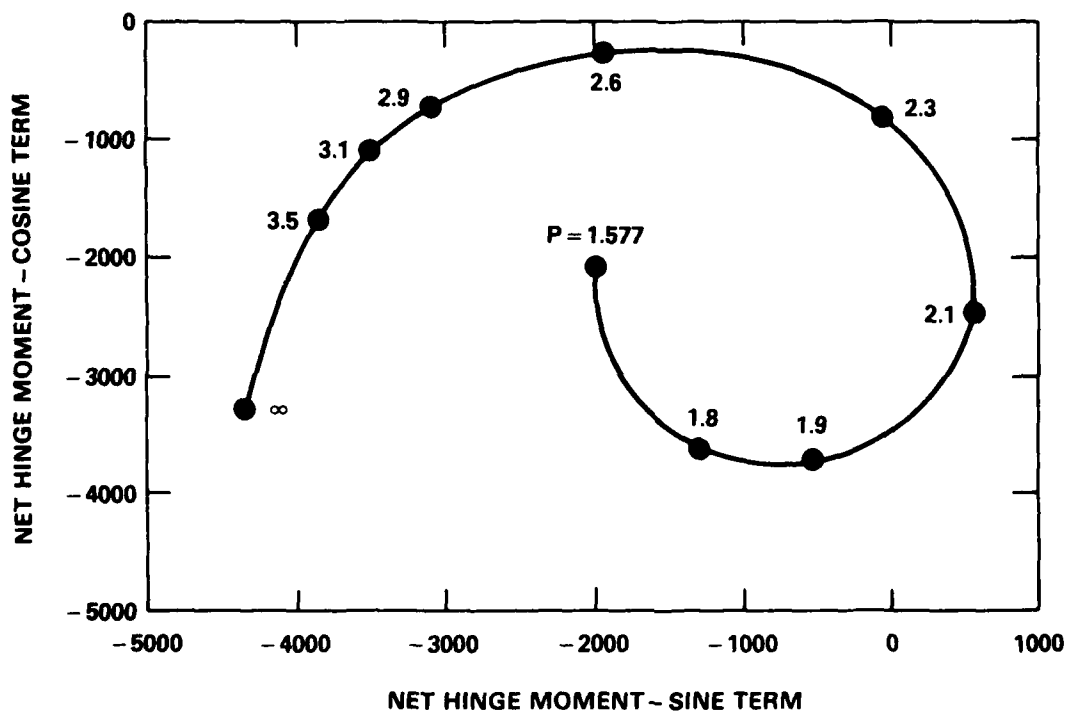


Figure 9 - Cross Plot of Net Hinge Moment Components

APPLICATION TO ROTOR PERFORMANCE ANALYSIS

HUB MOMENTS

To evaluate rotor hub moments properly, the flapping solution must be used. Flapping motion changes the azimuth angle where the combined aerodynamic and

inertia loads are passed back through the hinge to the hub. Referring to Figure 1, the hub moment is:

$$HM(\psi) = \int_0^{r_0} r(d\ell/dr)dr + r_0 \int_{r_0}^R (d\ell/dr)dr + k \beta(\psi) - r_0 m \ddot{\beta}(\psi) \quad (11)$$

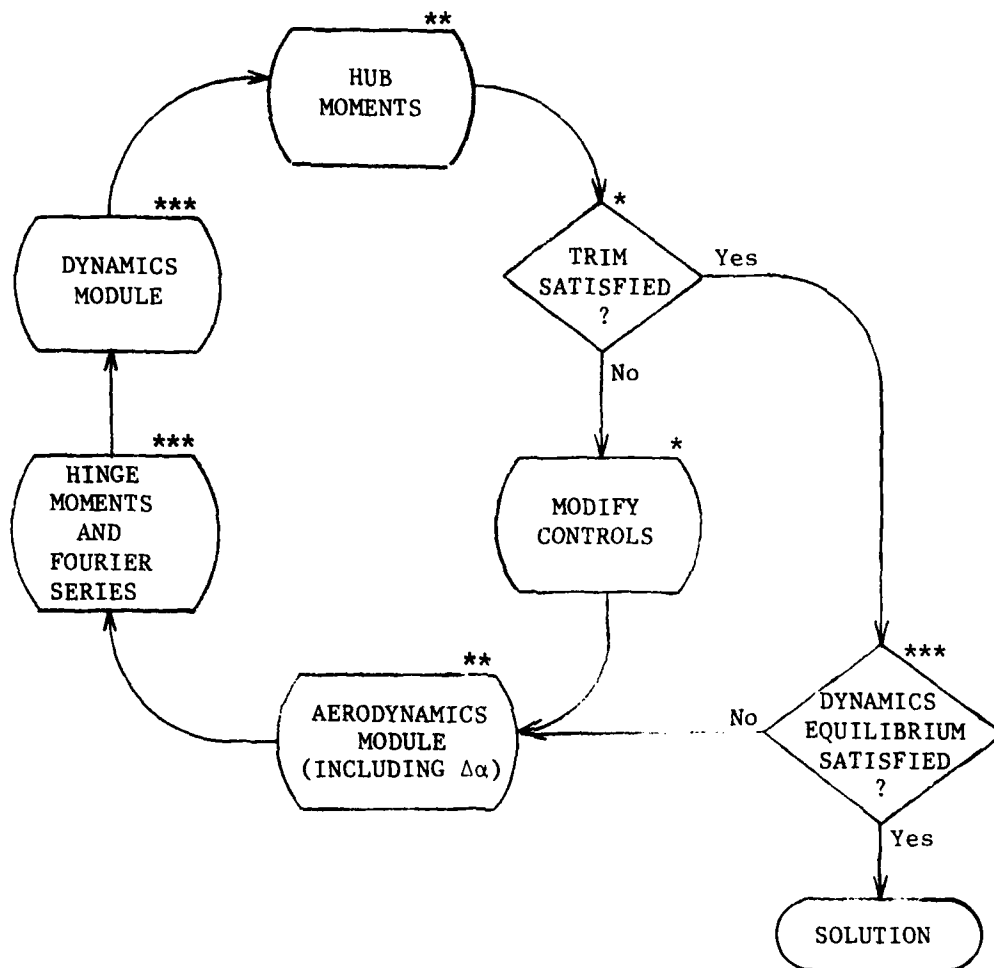
The first term is the hub moment due to aerodynamic lift inboard of the hinge, if any. The second term is the hub moment from the shear force acting at the hinge. The third term is the moment passed across the hinge spring; the fourth term is the inertial shear at the hinge. These terms implicitly account for all of the inertia, lift, and centrifugal forces acting on the blade, as reflected in the flapping angle solution β . If the hinge is a pure pin (no spring), then $k=0$, and no hinge moment exists. Thus, flapping changes the hub moment by modifying the aerodynamic load through the $\dot{\beta}$ influence and by introducing dynamic terms.

SOLUTION

The XWDYN dynamics module may be added to a rotor aerodynamics program in a general (modular) way, thus allowing for more elaborate flapping solutions in the future. Figure 10 outlines a technique where the specific airload-to-flap relation is accounted for in the dynamics module. As described, the module basically would be that of Equation (10). Other necessary modifications to the main program, for this or any other dynamics module, include:

- Providing for dynamic characteristics in main I/O routine
- Calculating the aerodynamic hinge moment versus azimuth, $M_h(\psi)$
- Using Fourier series for $M_h(\psi)$
- Adding $\Delta\alpha$ term due to $\dot{\beta}$ in aerodynamic loads
- Adding a dynamic equilibrium check
- Changing hub moment calculations to reflect the dynamic module

The advantage in using this solution is that it is easily added to an existing main program. While more elaborate techniques may be used, this technique has the least impact on the original main program. The modular approach allows future improvements to the flapping representation.



- * Existing
- ** Requires Modification
- *** New Module

Figure 10 - Modular Inclusion of Rotor Blade Dynamics

SUMMARY

A relatively simple relationship has been derived to allow calculation of the first three harmonics of blade flapping response to the specified first three harmonics of aerodynamic hinge moments. This relationship was developed as a computer program dynamics module, XWDYN. This module can be easily incorporated into existing rotor aerodynamic analyses to account for the first-order influence of blade flapping response. The XWDYN dynamics module has been validated by comparing results with those from another analytical technique.

A brief study was made to evaluate the potential influence of blade dynamics on the solution of an X-Wing conversion case. Results show high 2/rev blade response for the particular case examined ($\mu = 0.7$). The magnitude and phase angle of response change dramatically with changes in the first flap frequency of the blade. In particular, this response shows a strong influence on both the 2/rev flapping and on the first harmonic of net hinge moment, suggesting a frequency influence on rotor cyclic control effectiveness. This effect should be examined further by incorporating the XWDYN module into a rotor aerodynamics routine for a complete iterative solution.

DTNSRDC ISSUES THREE TYPES OF REPORTS

1. DTNSRDC REPORTS, A FORMAL SERIES, CONTAIN INFORMATION OF PERMANENT TECHNICAL VALUE. THEY CARRY A CONSECUTIVE NUMERICAL IDENTIFICATION REGARDLESS OF THEIR CLASSIFICATION OR THE ORIGINATING DEPARTMENT.

2. DEPARTMENTAL REPORTS, A SEMIFORMAL SERIES, CONTAIN INFORMATION OF A PRELIMINARY, TEMPORARY, OR PROPRIETARY NATURE OR OF LIMITED INTEREST OR SIGNIFICANCE. THEY CARRY A DEPARTMENTAL ALPHANUMERICAL IDENTIFICATION.

3. TECHNICAL MEMORANDA, AN INFORMAL SERIES, CONTAIN TECHNICAL DOCUMENTATION OF LIMITED USE AND INTEREST. THEY ARE PRIMARILY WORKING PAPERS INTENDED FOR INTERNAL USE. THEY CARRY AN IDENTIFYING NUMBER WHICH INDICATES THEIR TYPE AND THE NUMERICAL CODE OF THE ORIGINATING DEPARTMENT. ANY DISTRIBUTION OUTSIDE DTNSRDC MUST BE APPROVED BY THE HEAD OF THE ORIGINATING DEPARTMENT ON A CASE-BY-CASE BASIS.